The Canadian Mineralogist
Vol. 42, pp. 825-834 (2004)

THE CRYSTAL STRUCTURE OF HUBEITE, A NOVEL SOROSILICATE MINERAL

MARK A. COOPER AND FRANK C. HAWTHORNE[§]

Department of Geological Sciences, University of Manitoba, Winnipeg, Manitoba R3T 2N2, Canada

ABSTRACT

The crystal structure of hubeite, $Ca_2\,Mn^{2+}\,Fe^{3+}\,[Si_4\,O_{12}\,(OH)]\,(H_2O)_2$, triclinic, space group $P\bar{1}$, *a* 9.9653(3), *b* 13.9171(3), *c* 6.5703(2) Å, α 133.264(1), β 101.414(1), γ 66.302(1)°, *V* 603.47(6) Å^3, *Z* = 2, has been solved by direct methods and has been refined to an *R* index of 2.2% based on 2875 observed (5σ) reflections measured with Mo*K*α X-radiation. There are two *Ca* sites, one [8]- and one [7]-coordinated, with <*Ca*–ϕ> (ϕ: O, OH, H_2O) distances of 2.527 and 2.485 Å, respectively. There is one *Mn* site octahedrally coordinated by five O-atoms and one (OH) group, with a <*Mn*–O> distance of 2.224 Å, indicating occupancy of this site by Mn^{2+}. There is one *Fe* site octahedrally coordinated by O-atoms, with an <*Fe*–O> distance of 2.025 Å, indicating occupancy of this site by Fe^{3+}. There are four *Si* sites, each occupied solely by Si, with a <*Si*–O> distance of 1.627 Å. One of the silicate tetrahedra is an acid silicate group: $SiO_3(OH)$. The four *Si* tetrahedra link by sharing corners to form a linear $[Si_4\phi_{13}]$ group, and hence hubeite is a sorosilicate. The overall structure consists of layers of $[Si_4\phi_{13}]$ groups alternating with layers of edge-sharing [6]-, [7]- and [8]-coordinated Ca, Mn^{2+} and Fe^{3+} polyhedra parallel to (001). These layers stack in the [001] direction, forming a framework with tunnels that extend along [001] and contain the isolated (H_2O) groups. The structure of hubeite is related to the structures of inesite, rhodonite and babingtonite.

Keywords: hubeite, crystal structure, sorosilicate, Hubei, China.

SOMMAIRE

Nous avons résolu la structure cristalline de la hubéite, $Ca_2\,Mn^{2+}\,Fe^{3+}\,[Si_4\,O_{12}\,(OH)]\,(H_2O)_2$, triclinique, groupe spatial $P\bar{1}$, *a* 9.9653(3), *b* 13.9171(3), *c* 6.5703(2) Å, α 133.264(1), β 101.414(1), γ 66.302(1)°, *V* 603.47(6) Å^3, *Z* = 2, par méthodes directes, et nous l'avons affiné jusqu'à un résidu *R* de 2.2% en utilisant 2875 réflexions observées (5σ) mesurées avec rayonnement Mo*K*α. Il y a deux sites *Ca*, un à coordinence [8] et le second à coordinence [7], avec une distance <*Ca*–ϕ> (ϕ: O, OH, H_2O) de 2.527 et 2.485 Å, respectivement. Il y a un site *Mn* à coordinence octaédrique impliquant cinq atomes d'oxygène et un groupe (OH), avec une distance <*Mn*–O> de 2.224 Å, indication de la présence de Mn^{2+}. La structure contient un site *Fe* à coordinence octaédrique impliquant des atomes d'oxygène, la distance <*Fe*–O> étant 2.025 Å, indication de la présence de Fe^{3+} à ce site. Il y a quatre sites *Si*, chacun contenant le Si seulement, avec une distance <*Si*–O> de 1.627 Å. Un des tétraèdres est une groupe silicate acide: $SiO_3(OH)$. Les quatre tétraèdres *Si* sont interliés par partage de coins, pour former un agencement linéaire $[Si_4\phi_{13}]$; c'est donc dire que la hubéite est un sorosilicate. La structure est faite de couches de groupes $[Si_4\phi_{13}]$ en alternance avec des couches de polyèdres à arêtes partagées parallèles à (001), contenant le Ca, Mn^{2+} et Fe^{3+} en coordinence [6], [7] et [8]. Ces feuillets sont empilés le long de [001] pour former une trame ayant des tunnels le long de [001] qui contiennent des groupes isolés de (H_2O). La structure de la hubéite ressemble à celle de l'inésite, de la rhodonite et de la babingtonite.

(Traduit par la Rédaction)

Mots-clés: hubéite, structure cristalline, sorosilicate, Hubei, Chine.

[§] *E-mail address*: frank_hawthorne@umanitoba.ca

INTRODUCTION

Hubeite was described as a new mineral species by Hawthorne *et al.* (2002). It was discovered at the Daye Fe–Cu–Au mines, Huangshi, Hubei province, China, where it is associated in a skarn assemblage with pink inesite, colorless apophyllite, quartz, pyrite and colorless to white calcite. The formula of hubeite, $Ca_2\,Mn^{2+}\,Fe^{3+}\,[Si_4O_{12}(OH)]\,(H_2O)_2$, suggests that it is a sorosilicate.

EXPERIMENTAL

The crystals used in this work are from the type locality and were obtained from Mr. Charles L. Key. A small crystal was attached to a glass fiber and mounted on a Siemens *P*4 automated four-circle diffractometer equipped with a 1 K CCD detector and Mo*K*α X-radiation. The settings of 6254 ($>10\ I\,/\,\sigma$) reflections were used to refine the unit-cell dimensions by least-squares (Table 1). Intensity data were collected using a frame width of 0.2° and a frame time of 45 s, and 10,074 reflections were integrated over the range $4 \leq 2\theta \leq 60°$. The data were corrected for absorption using SADABS, and for Lorentz, polarization and background effects, averaged and reduced to structure factors; of the 3456 unique reflections, 2875 reflections were considered as observed [$|F_o| \geq 5\sigma F$].

STRUCTURE SOLUTION AND REFINEMENT

Scattering curves for neutral atoms were taken from the International Tables for Crystallography (Ibers & Hamilton 1992). *R* indices are given in Table 1, and are expressed as percentages. The Siemens SHELXTL PLUS (PC version) system of programs was used for this work.

The structure refined rapidly to an *R* index of ~3% for a model with variable scattering at the cation sites with coordination numbers between [6] and [8], and anisotropic displacements on all non-H atoms. The occupancies at the *Fe* and *Mn* sites refined to values marginally less than their ideal sums for these sites, consistent with the presence of minor "lighter" scattering species at both sites. Minor Al and Mg from the chemical analysis was assigned to the *Fe* site, and the amount of Ca in excess of 2 atoms per formula unit (*apfu*) was assigned to the *Mn* site (Table 2), in accord with the observed scattering and bond lengths at the two sites. The OW(2) and OW(3) sites are each half occupied by (H_2O) groups [separation = 0.69(1) Å]. Hydrogen positions were located in the difference-Fourier map and included in the model with the soft constraint that they lie approximately 0.98 Å from their respective donor O-atom. Full-matrix least-squares refinement of all variable parameters for a model involving anisotropic displacement of all non-H atoms converged to an *R* index of 2.2% for 2875 unique observed reflections.

Positional and displacement parameters for the refinement are given in Table 3, selected interatomic distances and angles in Table 4, and a bond-valence analysis in Table 5. Observed and calculated structure-factors are available from The Depository of Unpublished Data, CISTI, National Research Council, Ottawa, Ontario K1A 0S2, Canada.

ELECTRON-MICROPROBE ANALYSIS

The crystal used in the collection of the X-ray intensity data was analyzed after the X-ray work with a Cameca SX–50 electron microprobe operating in wavelength-dispersion mode with an accelerating voltage of 15 kV, a specimen current of 20 nA, a beam size of

TABLE 1. MISCELLANEOUS INFORMATION FOR HUBEITE

a (Å)	9.9653(3)	crystal size (μm)	40 x 200 x 200
b	13.9171(3)	radiation	Mo*K*α/Gr
c	6.5703(2)	No. of reflections	10074
α (°)	133.264(1)	No. in Ewald sphere	6129
β	101.414(1)	No. unique $\|F\|$	3456
γ	66.302(1)	No. $\|F_o\| > 5\sigma(\|F\|)$	2875
V (Å³)	603.47(6)	R_{merge} %	1.4
Sp. Gr.	$P\bar{1}$	*R* %	2.2
Z	2	wR %	2.5
μ (mm⁻¹)	3.59		
D_{meas} * (g/cm³)	3.02(2)		
D_{calc} (g/cm³)	3.01		

Cell content 2 $[Ca_2\,Mn^{2+}\,Fe^{3+}\,Si_4\,O_{12}\,(OH)\,(H_2O)_2]$

$R = \Sigma(|F_o| - |F_c|) / \Sigma|F_o|$

$wR = [\Sigma w(|F_o| - |F_c|)^2 / \Sigma (F_o^2)]^{½}$, $w = 1$

* from Hawthorne *et al.* (2002)

TABLE 2. CHEMICAL COMPOSITION (wt.%)* AND UNIT FORMULA** OF HUBEITE

SiO_2	44.48	Si	4.00
Al_2O_3	0.41		
Fe_2O_3	13.85	Fe^{3+}	0.94
MgO	0.27	Al	0.04
MnO	11.36	Mg	0.04
CaO	21.98	Σ	1.02
H_2O *	8.33		
Total	100.68	Mn^{2+}	0.87
		Ca	0.12
		Σ	0.99
		Ca	2.00
		OH	1
		H_2O	2

* calculated on the basis of 15 anions with OH = 1 and H_2O = 2 *apfu*

TABLE 3. ATOM POSITIONS AND DISPLACEMENT FACTORS FOR HUBEITE

	x	y	z	U_{11}	U_{22}	U_{33}	U_{23}	U_{13}	U_{12}	U_{eq}
Fe	0.12336(4)	0.89658(4)	0.01858(7)	0.00687(17)	0.00725(17)	0.00740(18)	0.00499(15)	0.00003(12)	–0.00184(12)	0.0073(2)
Mn	0.00897(4)	0.29187(4)	0.01555(8)	0.0094(2)	0.00972(18)	0.0108(2)	0.00763(16)	–0.00117(13)	–0.00333(13)	0.0094(3)
Ca(1)	0.61932(5)	0.36094(5)	0.00460(10)	0.0092(2)	0.0120(2)	0.0128(2)	0.0094(2)	–0.00026(16)	–0.00223(16)	0.0109(3)
Ca(2)	0.19528(5)	0.47015(5)	0.06104(11)	0.0107(2)	0.0173(2)	0.0191(3)	0.0150(2)	–0.00310(18)	–0.00588(18)	0.0131(3)
Si(1)	0.89574(7)	0.77879(7)	0.56898(14)	0.0099(3)	0.0083(3)	0.0083(3)	0.0058(3)	–0.0008(2)	–0.0033(2)	0.0087(4)
Si(2)	0.75432(7)	0.60786(7)	0.52352(14)	0.0077(3)	0.0094(3)	0.0091(3)	0.0067(3)	–0.0013(2)	–0.0035(3)	0.0083(4)
Si(3)	0.40783(7)	0.69102(7)	0.55270(14)	0.0074(3)	0.0094(3)	0.0093(3)	0.0068(3)	0.0002(2)	–0.0019(2)	0.0086(4)
Si(4)	0.18597(7)	0.92302(7)	0.57705(14)	0.0090(3)	0.0086(3)	0.0083(3)	0.0058(3)	0.0002(2)	–0.0023(2)	0.0087(4)
O(1)	0.8064(2)	0.94162(18)	0.6974(4)	0.0129(8)	0.0093(7)	0.0122(8)	0.0077(7)	–0.0013(6)	–0.0035(6)	0.0112(11)
O(2)	–0.0118(2)	0.23117(18)	0.2302(4)	0.0134(8)	0.0123(8)	0.0124(8)	0.0096(7)	–0.0028(6)	–0.0050(6)	0.0117(11)
O(3)	0.9692(2)	0.66894(18)	0.2470(4)	0.0153(8)	0.0110(8)	0.0085(8)	0.0063(7)	0.0006(6)	–0.0024(6)	0.0126(11)
O(4)	0.7629(2)	0.7315(2)	0.5521(4)	0.0144(8)	0.0151(8)	0.0217(9)	0.0146(8)	–0.0054(7)	–0.0083(7)	0.0145(12)
O(5)	0.7962(2)	0.46530(18)	0.1929(4)	0.0136(8)	0.0115(8)	0.0093(8)	0.0061(7)	–0.0015(6)	–0.0047(6)	0.0123(11)
O(6)	0.8498(2)	0.5950(2)	0.7331(4)	0.0122(8)	0.0169(8)	0.0140(8)	0.0125(7)	–0.0026(6)	–0.0057(7)	0.0125(12)
O(7)	0.5808(2)	0.6530(2)	0.5999(4)	0.0082(8)	0.0256(10)	0.0244(10)	0.0204(9)	–0.0020(7)	–0.0047(7)	0.0168(14)
O(8)	0.3926(2)	0.55596(18)	0.2402(4)	0.0127(8)	0.0115(8)	0.0105(8)	0.0063(7)	–0.0009(6)	–0.0033(6)	0.0131(11)
O(9)	0.3155(2)	0.74208(18)	0.8054(4)	0.0106(8)	0.0135(8)	0.0125(8)	0.0099(7)	0.0015(6)	–0.0022(6)	0.0116(11)
O(10)	0.3543(2)	0.8183(2)	0.5472(4)	0.0109(8)	0.0135(8)	0.0177(9)	0.0125(8)	0.0014(6)	–0.0013(6)	0.0130(12)
O(11)	0.1478(2)	0.84494(18)	0.2563(4)	0.0127(8)	0.0111(7)	0.0093(8)	0.0065(7)	–0.0007(6)	–0.0041(6)	0.0114(11)
O(12)	0.08130(18)	0.94486(18)	0.7725(4)	0.0100(8)	0.0100(7)	0.0109(8)	0.0072(7)	0.0020(6)	–0.0016(6)	0.0104(11)
OH	0.1938(2)	0.07417(18)	–0.2791(4)	0.0181(9)	0.0096(8)	0.0116(8)	0.0069(7)	–0.0005(7)	–0.0056(7)	0.0129(11)
OW(1)	0.4280(2)	0.2521(2)	–0.1743(4)	0.0196(9)	0.0191(9)	0.0182(10)	0.0111(8)	–0.0015(8)	–0.0090(8)	0.0195(13)
OW(2)	0.5137(7)	0.0159(7)	–0.2640(12)	0.0171(27)	0.0242(26)	0.0360(32)	0.0163(29)	–0.0060(25)	–0.0110(19)	0.0287(41)
OW(3)	0.5080(8)	0.0445(8)	–0.1273(15)	0.0202(27)	0.0471(42)	0.0569(46)	0.0287(44)	–0.0069(34)	–0.0117(27)	0.0483(61)
H(1)	0.205(4)	0.070(4)	–0.430(5)							0.0296(100)
H(2)	0.425(5)	0.190(4)	–0.3781(15)							0.0500*
H(3)	0.456(5)	0.179(4)	–0.165(10)							0.0500*
H(4)	0.6117(4)	–0.003(4)	–0.204(5)							0.0500*
H(5)	0.459(4)	–0.024(4)	–0.248(4)							0.0500*

* fixed in refinement

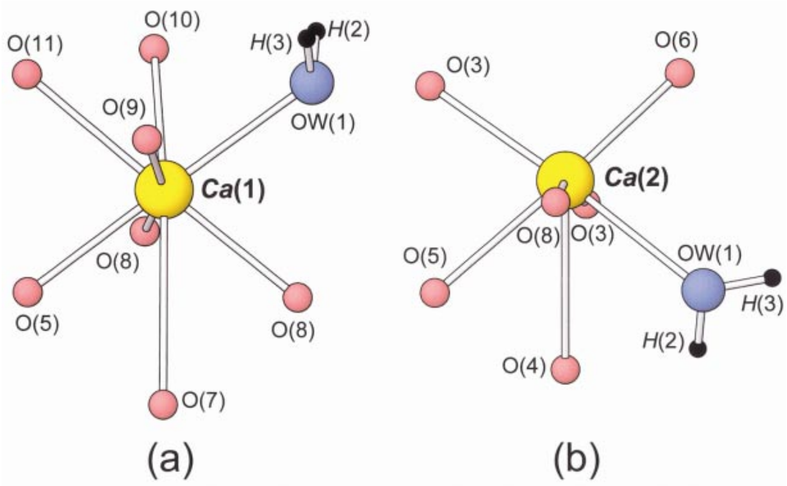

FIG. 1. The Ca coordination in hubeite: (a) *Ca*(1); (b) *Ca*(2). Ca atoms are shaded yellow circles, O atoms are shaded brown circles, (H_2O) groups are shaded blue (O-atom) and black (H-atom) circles.

TABLE 4. SELECTED INTERATOMIC DISTANCES (Å) AND ANGLES IN HUBEITE

Fe–O(1)a	2.008(2)	*Mn*–O(2)	2.153(3)
Fe–O(2)b	1.989(2)	*Mn*–O(3)e	2.203(3)
Fe–O(9)c	1.969(1)	*Mn*–O(5)f	2.165(2)
Fe–O(11)	2.065(3)	*Mn*–O(6)g	2.118(2)
Fe–O(12)c	2.058(3)	*Mn*–O(11)b	2.425(2)
Fe–O(12)d	2.062(1)	*Mn*–OH	2.281(1)
<*Fe*–O>	2.025	<*Mn*–φ>	2.224
Ca(1)–O(5)	2.341(2)	*Ca*(2)–O(3)f	2.381(2)
Ca(1)–O(7)	3.084(2)	*Ca*(2)–O(3)e	2.529(2)
Ca(1)–O(8)	2.358(2)	*Ca*(2)–O(4)e	2.916(2)
Ca(1)–O(8)e	2.510(3)	*Ca*(2)–O(5)e	2.402(3)
Ca(1)–O(9)g	2.328(3)	*Ca*(2)–O(6)g	2.259(4)
Ca(1)–O(10)e	2.625(2)	*Ca*(2)–O(8)	2.393(2)
Ca(1)–O(11)e	2.456(1)	*Ca*(2)–OW(1)	2.512(2)
Ca(1)–OW(1)	2.512(3)	<*Ca*(2)–φ>	2.485
<*Ca*(1)–φ>	2.527		
Si(1)–O(1)	1.641(2)	*Si*(3)–O(7)	1.620(2)
Si(1)–O(2)g	1.617(2)	*Si*(3)–O(8)	1.608(2)
Si(1)–O(3)	1.621(2)	*Si*(3)–O(9)	1.603(3)
Si(1)–O(4)	1.655(3)	*Si*(3)–O(10)	1.657(3)
<*Si*(1)–O>	1.634	<*Si*(3)–O>	1.622
Si(2)–O(4)	1.635(3)	*Si*(4)–O(10)	1.658(2)
Si(2)–O(5)	1.617(2)	*Si*(4)–O(11)	1.626(2)
Si(2)–O(6)	1.586(3)	*Si*(4)–O(12)	1.603(3)
Si(2)–O(7)	1.636(2)	*Si*(4)–OHh	1.644(3)
<*Si*(2)–O>	1.619	<*Si*(4)–φ>	1.633
Si(1)–O(4)–*Si*(2)	135.7(1)		
Si(2)–O(7)–*Si*(3)	153.4(2)		
Si(3)–O(10)–*Si*(4)	130.1(2)		

a: $1-x, 2-y, 1-z$; b: $\bar{x}, 1-y, \bar{z}$; c: $x, y, z-1$; d: $\bar{x}, 2-y, 1-z$; e: $1-x, 1-y, \bar{z}$; f: $x-1, y, z$; g: $1-x, 1-y, 1-z$; h: $x, 1+y, 1+z$

2 μm and counting times on peak and background of 20 and 10 s, respectively. The following standards were used: diopside (Si, Ca); spessartine (Mn); fayalite (Fe); andalusite (Al); forsterite (Mg). Data were reduced using the $\phi(\rho Z)$ procedure of Pouchou & Pichoir (1985). The chemical composition of the fragment used in the collection of the X-ray intensity data is given in Table 2 and is the mean of 10 determinations. The unit formula was calculated on the basis of fifteen anions including one (OH) and two (H_2O) groups.

DESCRIPTION OF THE STRUCTURE

Coordination of the cations

There are two *Ca* sites, each occupied entirely by Ca. The *Ca*(1) site is coordinated by seven O-atoms between 2.328 and 2.625 Å and one O-atom at 3.084 Å arranged at the vertices of a distorted cube (Fig. 1a). The *Ca*(2) site is coordinated by six O-atoms between 2.259 and 2.529 Å and one O-atom at 2.916 Å arranged at the vertices of an augmented octahedron (Fig. 1b). There are four *Si* sites, each occupied by Si and surrounded by four anions in a tetrahedral arrangement. The <*Si*–O> distances are typical for Si, and are in accord with the absence of $^{[4]}$Al in hubeite. Note that *Si*(4) bonds to an (OH) group, and hence the resultant tetrahedron is an acid-silicate group: $SiO_3(OH)$. The O(4) and O(7) anions bridge two Si atoms, and hubeite is a sorosilicate. The only other known sorosilicate containing an [$Si_4\phi_{13}$] group is ruizite, where the Si tetrahedra contain only Si and link *via* two unique bridging O-atoms [O_{br}] (Hawthorne 1984). In ruizite, one of the O_{br} anions is involved in a weak bond (0.17 *vu*) to Ca (Ca–O_{br} = 2.613 Å), and the other O_{br} is coordinated by two Si atoms only. The bond valence at the O_{br} anion from the Si–O_{br} bonds is shown as a function of the bond-valence incident from the Ca–O_{br} bond for both ruizite and hubeite in Figure 2. The near-linear relation indicates that the assigned weak Ca–O_{br} bonds in hubeite are conformable with the overall bond-valence requirements for the O_{br} anion.

There is one *Fe* site surrounded by six O-atoms in an octahedral arrangement with an <*Fe*–O> distance of 2.025 Å. This value is close to the sum of the empirical radii (Shannon 1976) for the constituent species: $^{[3\frac{1}{3}]}$O + $^{[6]}$Fe^{3+} = 1.36 + 0.645 = 2.012 Å, indicating that Fe is present in the trivalent state. There is one *Mn* site surrounded by five O-atoms and one (OH) group in an octahedral arrangement with an <*Mn*–O> distance of 2.224 Å. This value is close to the sum of the empirical radii for the constituent species $^{[3\frac{1}{3}]}$O + $^{[6]}$Mn^{2+} = 1.37 + 0.83 = 2.20 Å, indicating that Mn is present in the divalent state.

Structure topology

The structure of hubeite is a framework of heteropolyhedra with alternating layers of tetrahedra and [6]-, [7]- and [8]-coordination polyhedra parallel to (001).

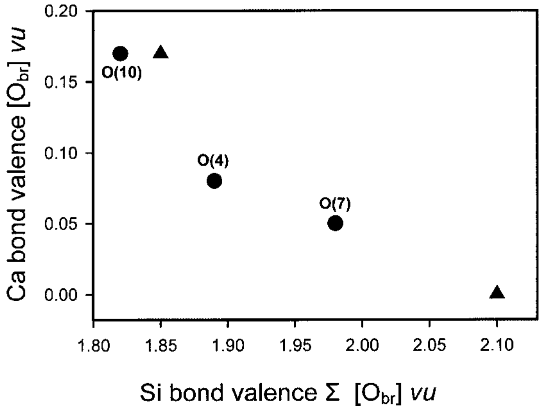

FIG. 2. Variation in bond-valence at the bridging O-atom (O_{br}) from the Si–O_{br} bonds as a function of the bond-valence incident from the Ca–O_{br} bond, for ruizite (shaded triangles) and hubeite (shaded circles).

TABLE 5. BOND-VALENCE* TABLE (*vu*) FOR HUBEITE

	Ca(1)	*Ca*(2)	*Fe*	*Mn*	*Si*(1)	*Si*(2)	*Si*(3)	*Si*(4)	Σ	H(1)	H(2)	H(3)	H(4)	H(5)	Σ
O(1)			0.51		0.96				1.47	0.25			0.15		1.87
O(2)			0.54	0.37	1.02				1.93						1.93
O(3)		0.33 0.22		0.33	1.01				1.89						1.89
O(4)		0.08			0.92	0.97			1.97		$^{\times1/2}\downarrow 0.10^{\times1/2}\rightarrow$				2.02
O(5)	0.36	0.31		0.36		1.02			2.05						2.05
O(6)		0.45		0.41		1.11			1.97						1.97
O(7)	0.05					0.97	1.01		2.03						2.03
O(8)	0.35 0.23	0.32					1.04		1.94						1.94
O(9)	0.38		0.57				1.06		2.01						2.01
O(10)	0.17						0.91	0.91	1.99					0.10	2.09
O(11)	0.27		0.44	0.18				0.99	1.88						1.88
O(12)			0.45 0.44					1.06	1.95						1.95
OH				0.27				0.95	1.22	0.75					1.97
OW(1)	0.23	0.23							0.46		0.90	0.80			2.16
OW(2)**									0.00		$^{\times1/2}\downarrow 0.10$	$^{\times1/2}\downarrow 0.20$	0.85	0.90	2.05
OW(3)**									0.00			$^{\times1/2}\downarrow 0.20$	0.85	0.90	1.95
Σ	2.04	1.94	2.95	1.92	3.91	4.07	4.02	3.91		1.00	1.00	1.00	1.00	1.00	

* calculated using the curves of Brown & Altermatt (1985);
** half-occupied

The layer of tetrahedra: The four Si tetrahedra link *via* bridging O-atoms at O(4), O(7) and O(10) to form a near-planar crescent-shaped [$Si_4\phi_{13}$] group (Figs. 3a, b). The individual Si–O distances and Si–O_{br}–Si angles (Table 4) are similar to those in ruizite (Hawthorne 1984), and the correlation between increasing <Si–O_{br}> and Si–O_{br}–Si is also very similar (Fig. 4). The basic geometrical difference between the [$Si_4\phi_{13}$] groups in hubeite and ruizite is shown in Figure 5. The crescent-shaped [$Si_4\phi_{13}$] group in hubeite (Fig. 5b) can be approximately derived from the [$Si_4\phi_{13}$] group in ruizite (Fig. 5a) by 180° rotation about the midpoint of the latter group. Also note that ruizite contains two central acid $SiO_3(OH)$ tetrahedra, whereas hubeite contains a single $SiO_3(OH)$ tetrahedron at one end of the [$Si_4\phi_{13}$] group. Opposing [$Si_4\phi_{13}$] groups in hubeite, related through a center of symmetry, form eight-membered rings of tetrahedra internally linked by two strong hydrogen-bonds (Fig. 3c). Within the central cavity of the ring of tetrahedra are the isolated (H_2O) groups OW(2) and OW(3).

The layer of heteropolyhedra: The Ca polyhedra share edges to form a linear tetramer, and these tetramers share edges to form staggered ribbons that extend in the *a* direction (Fig. 6). The edges of these ribbons are decorated with Mn octahedra that share edges with the Ca polyhedra, and these ribbons are linked in the *b* direction by dimers of edge-sharing Fe octahedra (Fig. 6). The [$Si_4\phi_{13}$] groups occur around the large holes in the layer of heteropolyhedra, sharing corners with all types of di- and trivalent metal polyhedra. The resulting sheet has large holes (Fig. 6), and the sheets stack in the *c* direction, creating channels along [001] that are occupied by the isolated (H_2O) groups at OW(2) and OW(3) and by the H-atoms belonging to OW(1).

Hydrogen bonding

As noted above, the [$Si_4\phi_{13}$] group in hubeite contains a terminal $SiO_3(OH)$ tetrahedron in which the *H*(1) atom of the (OH) group forms a strong hydrogen bond to the O(1) anion of an adjacent [$Si_4\phi_{13}$] group, forming an interrupted eight-membered ring of tetrahedra (Figs. 3, 7, Tables 5, 6). The (H_2O) group at OW(1) is bonded to two Ca atoms and resides along the interior wall of the channel extending along [001] (Figs. 6, 7). The *H*(2) and *H*(3) atoms associated with OW(1) form hydrogen-bonds to the isolated (H_2O) groups OW(2) and OW(3). One (H_2O) *pfu* is equally distributed over the OW(2) and OW(3) sites such that each site is 50% occupied. The close proximity of OW(2) and OW(3) (0.69 Å) precludes mutual local occupancy of the two sites; however, note that the associated *H*(4) and *H*(5) sites are the same for both (H_2O) configurations. Each possible local hydrogen-bond configuration involving

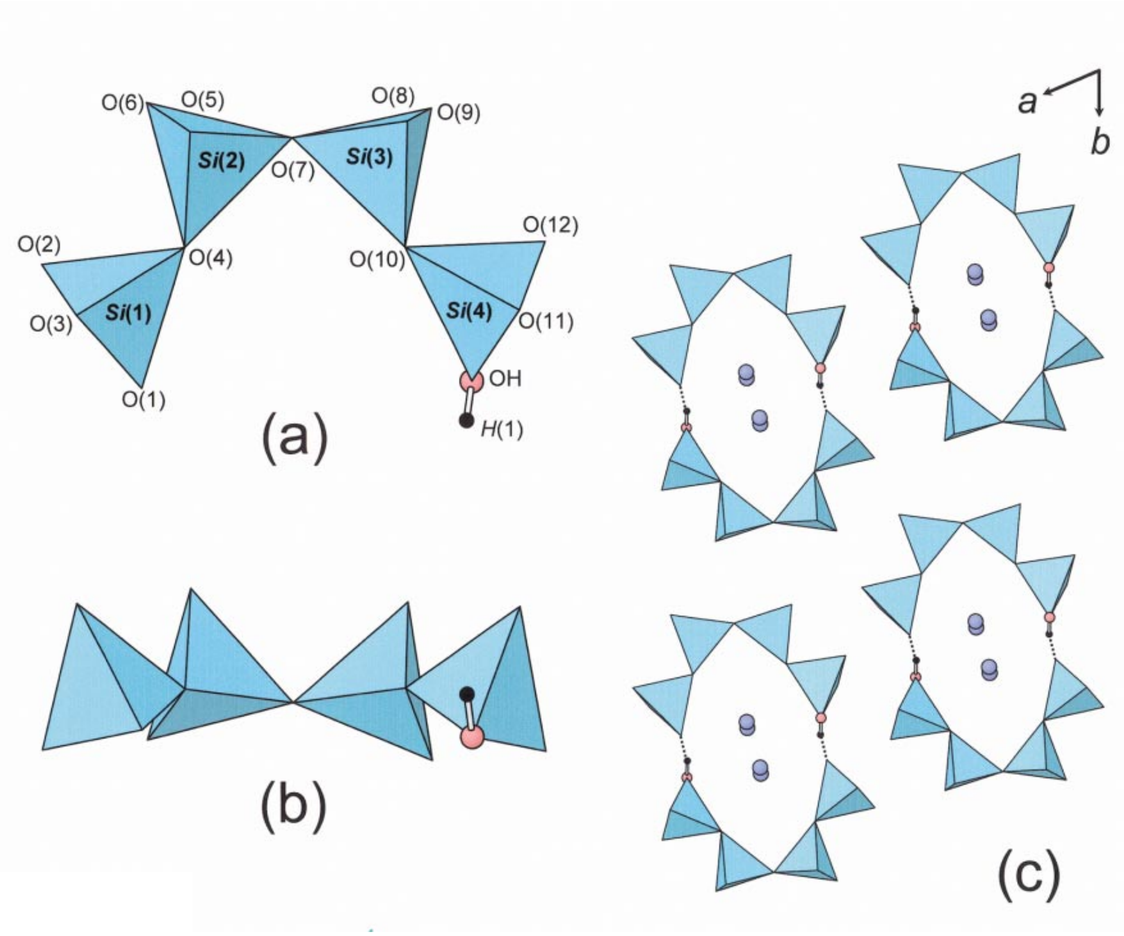

FIG. 3. The *Si* tetrahedra in hubeite: (a) plan view, and (b) side view of the [$Si_4\phi_{13}$] group; (c) the tetrahedron layer projected onto (001). Legend as in Figure 1; ($Si\phi_4$) tetrahedra are shaded blue, dashed lines are hydrogen bonds.

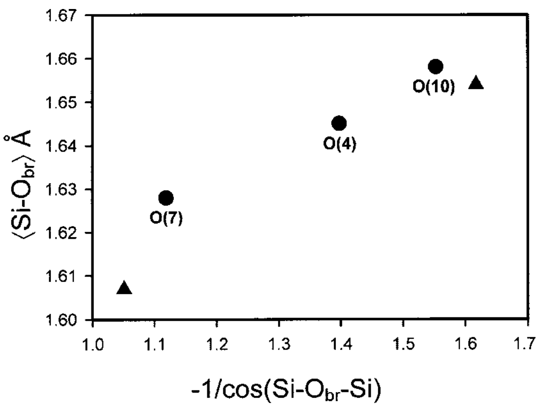

FIG. 4. Variation between <Si–O_{br}> and –1/cos(Si–O_{br}–Si). Legend as in Figure 2.

two adjacent OW(1) sites [and proximal OW(2)–OW(3) sites] is shown in Figure 7. Irrespective of whether OW(2) or OW(3) is locally occupied, the hydrogen bonds from the (H_2O) groups are invariably directed toward the O(1) and O(10) anions along the channel wall. The (H_2O) group in the channel may occur at two sites [OW(2)–OW(3)] along an axis [containing H(4) and H(5)] approximately perpendicular to *c*. The two sites occur owing to (1) the flexibility in the hydrogen bonding from the (H_2O) groups at OW(1), (2) the availability of sufficient room within the channel, and (3) a lack of mutual interference between OW(2) and OW(3) (H_2O) groups in the channel midway between pairs of OW(1) sites. Any of the three local arrangements shown in Figure 7 can occur next to each other along *c*. As a consequence of the last point, this degree of positional

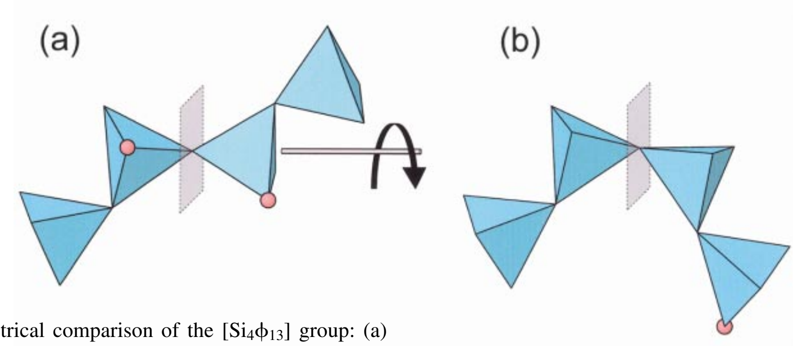

FIG. 5. Geometrical comparison of the [$Si_4\phi_{13}$] group: (a) ruizite; (b) hubeite. Legend as in Figure 3.

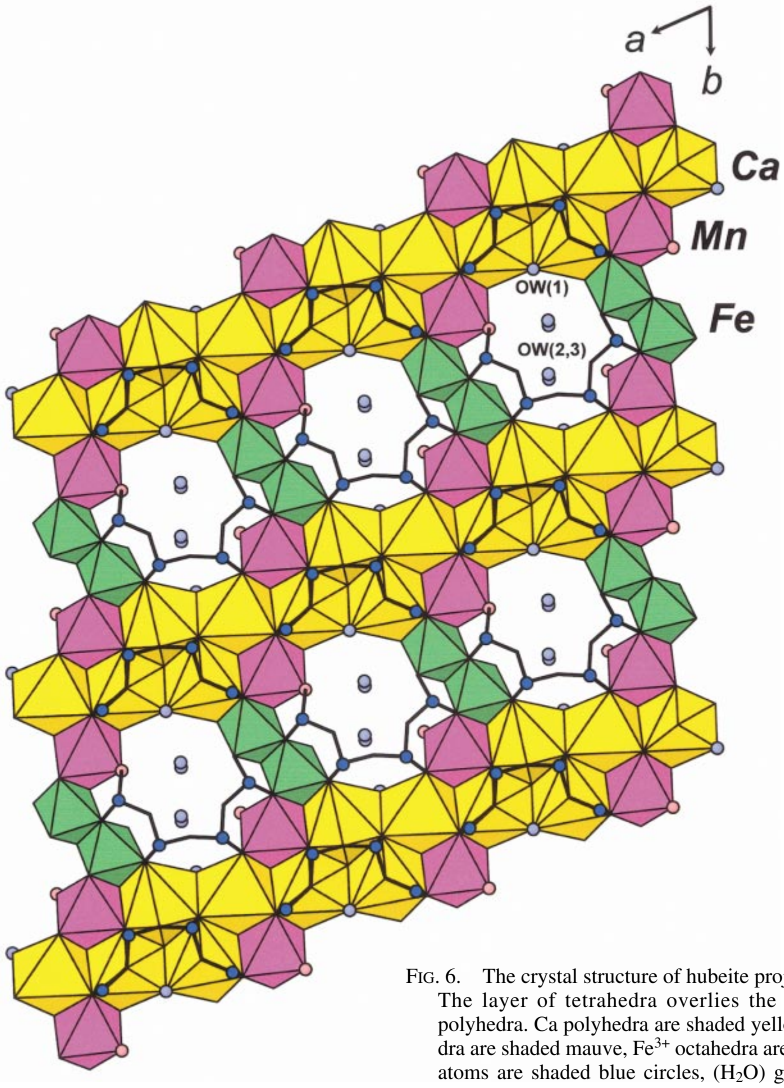

FIG. 6. The crystal structure of hubeite projected onto (001). The layer of tetrahedra overlies the layer of heteropolyhedra. Ca polyhedra are shaded yellow, Mn^{2+} octahedra are shaded mauve, Fe^{3+} octahedra are shaded green, Si atoms are shaded blue circles, (H_2O) groups are shaded light blue circles, (OH) groups are shaded brown circles. Thicker black lines are Si–ϕ bonds.

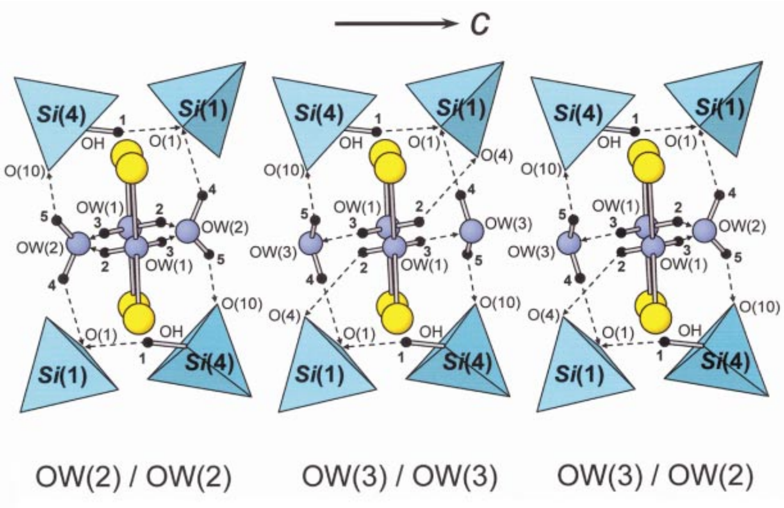

FIG. 7. The three possible local configurations of hydrogen bonds in hubeite. Legend as in Figures 1 and 3.

TABLE 6. HYDROGEN BONDING IN HUBEITE

OH–H(1)	0.98(5)	H(1)...O(1)e	1.63(5)
OH–O(1)e	2.603(4)	OH–H(1)–O(1)e	169(4)
OW(1)–H(2)	0.980(11)	H(2)...OW(2)i	2.01(3)
OW(1)–H(3)	0.98(7)	H(2)...O(4)e	2.29(4)
		H(3)...OW(2)	1.73(6)
OW(1)–OW(2)i	2.847(5)	H(3)...OW(3)	1.91(7)
OW(1)–O(4)e	2.897(4)		
OW(1)–OW(2)	2.677(10)	OW(1)–H(2)–OW(2)i	142(4)
OW(1)–OW(3)	2.890(14)	OW(1)–H(2)–O(4)e	119(3)
		OW(1)–H(3)–OW(2)	161(5)
H(2)–H(3)	1.47(8)	OW(1)–H(3)–OW(3)	177(5)
OW(2)–H(4)	0.980(17)	H(4)...O(1)j	1.840(18)
OW(2)–H(5)	0.98(6)	H(5)...O(10)j	2.23(5)
OW(2)–O(1)j	2.674(7)	OW(2)–H(4)–O(1)j	141(4)
OW(2)–O(10)j	3.111(10)	OW(2)–H(5)–O(10)j	150(2)
OW(3)–H(4)	0.980(13)	OW(3)–H(4)–O(1)j	170(4)
OW(3)–H(5)	0.98(5)	OW(3)–H(5)–O(10)j	168(4)
OW(3)–O(1)j	2.809(8)	H(4)–H(5)	1.60(6)
OW(3)–O(10)j	3.190(11)		

i: $1-x$, $\overline{y}$, $\overline{z}-1$; j: x, $y-1$, $z-1$

freedom suggests the possibility of dynamic disorder between OW(2) and OW(3) at room temperature.

RELATED STRUCTURES

Hubeite, inesite, babingtonite and rhodonite are all triclinic ($P\overline{1}$) minerals based on layers of edge-sharing (Ca–Mn–Fe) polyhedra that alternate with layers of Si tetrahedra (Table 7, Fig. 8). Rhodonite (Pertlik & Zahiri 1999) and babingtonite (Tagai *et al.* 1990) contain five-repeat chains of tetrahedra that, if artificially displaced in the manner shown by the red arrows in Figure 8, form alternating eight- and six-membered rings of tetrahedra analogous to those in inesite (Wan & Ghose 1978). If the two grey-shaded tetrahedra of the six-membered ring in inesite (Fig. 8) are omitted and the eight-membered ring is broken and hydroxylated, the arrangement of tetrahedra in hubeite is formed. The bands of polyhedra in rhodonite, babingtonite and inesite contain 10, 8 and 9 contiguous polyhedra, respectively, along the band, with relative offsets of 2, 0 and 1 octahedra on either side of

TABLE 7. RELATED MINERALS (FORMULA CONTENT ON A PER UNIT CELL BASIS)

	Rhodonite	Babingtonite	Inesite	Hubeite
tetrahedron layer	$[Si_{10}O_{30}]$	$[Si_{10}O_{28}(OH)_2]$	$[Si_{10}O_{28}]$	$[Si_8O_{24}(OH)_2]$
heteropolyhedral layer	$Mn^{2+}{}_8\ (Mn^{2+},Ca)_2$	$Ca_4\ Fe^{2+}{}_2\ Fe^{3+}{}_2$	$Ca_2\ Mn^{2+}{}_7\ (OH)_2\ (H_2O)_5$	$Ca_4\ Mn^{2+}{}_2\ Fe^{3+}{}_2\ (H_2O)_4$
σ_{calc}	3.69	3.36	3.02	3.01

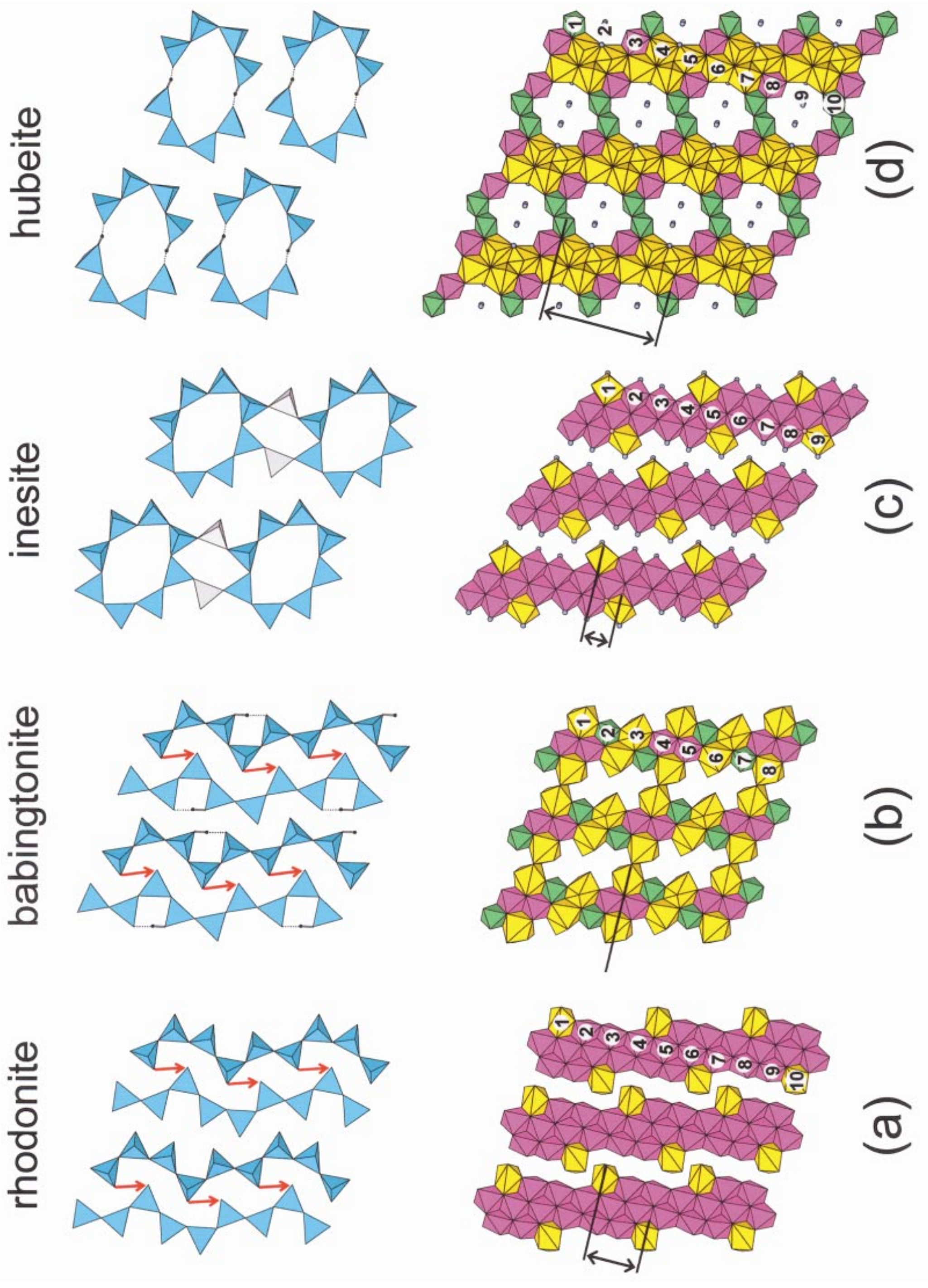

FIG. 8. The layers of tetrahedra and heteropolyhedra: (a) rhodonite projected onto ($\bar{1}1\bar{1}$); (b) babingtonite projected onto (101); (c) inesite projected onto ($1\bar{1}0$); (d) hubeite projected onto (001). The ($Si\phi_4$) tetrahedra are blue- and grey-shaded, the Ca-dominant polyhedra are shaded yellow, the Mn^{2+}- or Fe^{2+}-dominant (babingtonite) octahedra are shaded mauve, and the Fe^{3+}-dominant octahedra are shaded green. Red arrows indicate artificial displacement-vector. Black double-headed arrows mark relative offsets within the strips of polyhedra.

the central axis of the band. For hubeite, the strip of polyhedra is 10 polyhedra long; however, there are two vacancies near the ends of the strip. There is a greater degree of linkage of adjacent strips of polyhedra in hubeite (relative offset: four octahedra), with polyhedron vacancies in adjacent slabs arranged opposite each other, creating the large holes within the layer. The intimate physical association of hubeite and inesite at the Daye mines (Hawthorne *et al*. 2002) is not surprising, considering the close structural affinity (Fig. 8) , density and H_2O contents of these two minerals (Table 7).

ACKNOWLEDGEMENTS

We thank referees P.C. Burns and F. Pertlik, Associate Editor Nick Foit and Editor Bob Martin for their comments on this paper. FCH was supported by a Canada Research Chair in Crystallography and Mineralogy and by Major Facilities Access, Equipment and Discovery Grants from the Natural Sciences and Engineering Research Council of Canada.

REFERENCES

BROWN, I.D. & ALTERMATT, D. (1985): Bond-valence parameters obtained from a systematic analysis of the inorganic crystal structure database. *Acta Crystallogr.* **B41**, 244-247.

HAWTHORNE, F.C. (1984): The crystal structure of ruizite, a sorosilicate with an [$Si_4\phi_{13}$] cluster. *Tschermaks Mineral. Petrogr. Mitt.* **33**, 135-146.

________, COOPER, M.A., GRICE, J.D., ROBERTS, A.C., COOK, W.R. JR. & LAUF, R.I. (2002): Hubeite, a new mineral from the Daye mine near Huangshi, Hubei Province, China. *Mineral. Rec.* **33**, 465-471.

IBERS, J.A. & HAMILTON, W.C., eds. (1992): *International Tables for X-ray Crystallography* IV. Kynoch Press, Birmingham, U.K.

PERTLIK, F. & ZAHIRI, R. (1999): Rhodonite with a low calcium content: crystal structure determination and crystal chemical calculations. *Monatsh. Chem.* **130**, 257-265.

POUCHOU, J.L. & PICHOIR, F. (1985): "PAP" $\phi(\rho Z)$ procedure for improved quantitative microanalysis. *Microbeam Anal.* **1985**, 104–106.

SHANNON, R.D. (1976): Revised effective ionic radii and systematic studies of interatomic distances in halides and chalcogenides. *Acta Crystallogr.* **A32**, 751-767.

TAGAI, T., JOSWIG, W. & FUESS, H. (1990): Neutron diffraction study of babingtonite at 80 K. *Mineral. J.* **15**, 8-17.

WAN, CH'ENG & GHOSE, S. (1978): Inesite, a hydrated calcium manganese silicate with five-tetrahedral-repeat double chains. *Am. Mineral.* **63**, 563-571.

Received December 21, 2003, revised manuscript accepted March 15, 2004.